

Z = 50 Shell Gap near ^{100}Sn from Intermediate-Energy Coulomb Excitations in Even-Mass $^{106-112}\text{Sn}$ Isotopes

C. Vaman,¹ C. Andreoiu,² D. Bazin,¹ A. Becerril,^{1,3} B. A. Brown,^{1,3} C. M. Campbell,^{1,3} A. Chester,^{1,3} J. M. Cook,^{1,3} D. C. Dinca,^{1,3} A. Gade,^{1,3} D. Galaviz,¹ T. Glasmacher,^{1,3} M. Hjorth-Jensen,⁵ M. Horoi,⁶ D. Miller,^{1,3} V. Moeller,^{1,3} W. F. Mueller,¹ A. Schiller,¹ K. Starosta,^{1,3} A. Stolz,¹ J. R. Terry,^{1,3} A. Volya,⁴ V. Zelevinsky,^{1,3} and H. Zwahlen^{1,3}

¹National Superconducting Cyclotron Laboratory, Michigan State University, East Lansing, Michigan 48824, USA

²Department of Physics, University of Guelph, Guelph, Ontario N1G 2W1, Canada

³Department of Physics and Astronomy, Michigan State University, East Lansing, Michigan 48824, USA

⁴Physics Department, Florida State University, Tallahassee, Florida 32306, USA

⁵Department of Physics and Center of Mathematics for Applications, University of Oslo, N-0316, Oslo, Norway

⁶Department of Physics, Central Michigan University, Mount Pleasant, Michigan 48859, USA

(Received 22 November 2006; revised manuscript received 1 August 2007; published 15 October 2007)

Rare isotope beams of neutron-deficient $^{106,108,110}\text{Sn}$ from the fragmentation of ^{124}Xe were employed in an intermediate-energy Coulomb excitation experiment. The measured $B(E2, 0_1^+ \rightarrow 2_1^+)$ values for ^{108}Sn and ^{110}Sn and the results obtained for the ^{106}Sn show that the transition strengths for these nuclei are larger than predicted by current state-of-the-art shell-model calculations. This discrepancy might be explained by contributions of the protons from within the $Z = 50$ shell to the structure of low-energy excited states in this region.

DOI: 10.1103/PhysRevLett.99.162501

PACS numbers: 25.70.De, 23.20.Js, 23.20.Lv, 27.60.+j

While the concept of nuclear shell closures dates back to 1949 [1,2], it has not been until very recently that new tools have been developed which make further study of this topic possible. With the advent of rare isotope beams, experimental and theoretical efforts are currently focused on nuclear structure evolution far from the line of stability. In particular, the impact of the tensor interaction on the shell gaps [3] is a subject of lively discussion within the nuclear physics community. The isospin dependence of tensor interactions can give rise to so-called “monopole drifts” of specific single-particle subshells thus affecting the major shell closures. At the same time, the structure of excited states in neutron-deficient nuclei near the $N = Z$ line may be impacted by protons and neutrons occupying the same shell-model orbitals. This Letter reports observations which indicate that this might be, in fact, the case for neutron-deficient, even-mass, tin isotopes, near the doubly magic ^{100}Sn .

While experimental 2_1^+ state energies in $^{106-112}\text{Sn}$ are well established [4], the reduced probability for the electric quadrupole transition from the ground state to the first excited state, $B(E2, 0_1^+ \rightarrow 2_1^+)$, has been sparsely known except for stable Sn isotopes. For neutron-rich tin nuclei, the measurements of these $B(E2)$ values have only recently been achieved [5]. On the neutron-deficient side, the corresponding numbers are currently being reported, for ^{108}Sn from a recent intermediate-energy Coulomb excitation at GSI [6] and for ^{110}Sn from sub-barrier safe Coulomb excitation of Ref. [7]. The measurements on the neutron-deficient side of the $Z = 50$ chain are hindered by the 6_1^+ isomeric state with a lifetime in the nanosecond range, while the expected lifetime for the 2_1^+ state is at least 2 orders of magnitude shorter. Therefore, for a measurement,

the 2_1^+ state must be populated from the ground state. This Letter reports on the results of an intermediate-energy Coulomb excitation experiment with the neutron-deficient $^{106-110}\text{Sn}$ isotopes obtained from the fragmentation of ^{124}Xe . A measurement for ^{112}Sn is reported as a check of consistency with existing experimental data.

Beams of rare isotopes are produced via projectile fragmentation at the National Superconducting Cyclotron Laboratory (NSCL) as documented in Ref. [8]. In the current experiment a stable beam of ^{124}Xe was accelerated by the Coupled Cyclotron Facility to 140 MeV/nucleon and fragmented on a 300 mg/cm² thick Be foil at the target position of the A1900 fragment separator [9]. A combination of slits and a 165 mg/cm² Al wedge degrader were used at the A1900 to enhance the purity of the fragment of interest in the resulting cocktail beam. The properties of the Sn beams in this experiment are listed in Table I.

Coulomb excitation of the above cocktail beams on a 212 mg/cm² thick ^{197}Au target were studied using a combination of the Segmented Germanium Array (SeGA) [10] for γ -ray detection and the S800 spectrograph for particle identification and reconstruction of the reaction kinematics [11]. For all four tin isotopes studied, a lithium-like and a beryllium-like charge state were delivered to the S800

TABLE I. Sn beams used in the current experiment.

Isotope	Energy [MeV/u]	Purity [%]	$\Delta p/p$ [%]	Rate [10 ³ pps/pnA]
^{112}Sn	80	50	0.10	19
^{110}Sn	79	50	0.10	21
^{108}Sn	78	17	0.34	17
^{106}Sn	81	2	0.34	0.7

focal plane and identified by their position on the cathode readout drift chamber (CRDC) detectors [12]. The mass and charge of the nuclei were extracted on an event-by-event basis from the time of flight and energy loss information.

The S800 CRDC detectors measure position and angle in dispersive and nondispersive directions at the focal plane. This information can be used to reconstruct the trajectories of identified particles to the target position and to determine the impact parameter based on the knowledge of the magnetic field in the S800 [11,13]. This information is crucial to relate the Coulomb excitation cross section at the intermediate energies to the reduced $E2$ transition probability. For the projectile excitation this relation is given by Ref. [14]:

$$\sigma_{\text{proj}}(E2, I_i \rightarrow I_f) \propto B(E2, I_i \rightarrow I_f) Z_{\text{tar}}^2 / b_{\text{min}}^2, \quad (1)$$

where b_{min} is the minimum impact parameter considered for the cross section measurement. The minimum impact parameter is chosen to be large enough to minimize the interference of the nuclear force. The procedure outlined above has been applied in a number of successful experiments at the NSCL [14–16].

In the current study the absolute Coulomb excitation cross section measurement was hindered by a loss of CRDC efficiency for certain θ angles. Therefore, the experimental information on the transition rates is extracted from a relative measurement to excitations of the ^{197}Au target. Following Eq. (1), the ratio of the cross sections for the Sn projectile and Au target excitations in the current experiment is given by

$$\frac{\sigma_{\text{Sn}}(E2, 0_1^+ \rightarrow 2_1^+)}{\sigma_{\text{Au}}(E2, 3/2_1^+ \rightarrow 7/2_1^+)} = \frac{B_{\text{Sn}}(E2, 0_1^+ \rightarrow 2_1^+)}{B_{\text{Au}}(E2, 3/2_1^+ \rightarrow 7/2_1^+)} \left(\frac{79}{50}\right)^2 \quad (2)$$

The dependence on b_{min} , reaction kinematics and detector efficiencies in this ratio is removed, as long as safe COULEX conditions are met. The ratio of the cross sections is measured from the ratio of γ -ray intensities depopulating the 2_1^+ state in Sn and the $7/2_1^+$ state in the Au nuclei. Knowing the target $B(E2)$ [17] the corresponding transition rate for the projectile is extracted.

In view of the above, the analysis of the $^{108-112}\text{Sn}$ data proceeded in the following way. A subset of particle-identified events with the impact parameter larger than 19.5 fm was selected; the corresponding measured scattering angle in the lab was 45 mrad. Next, the cross section ratio measurements were performed according to Eq. (2) for the downstream ring at 37° and the ring at 90° separately, and the $B(E2)$'s in Sn nuclei were extracted from these ratios. Spectra illustrating the quality of the data for the 90° ring are shown in Fig. 1. The corresponding results are listed in Table II.

The ^{106}Sn measurement was most affected by the CRDC problems. Absence of reliable angle information for a significant fraction of the collected data required a relaxa-

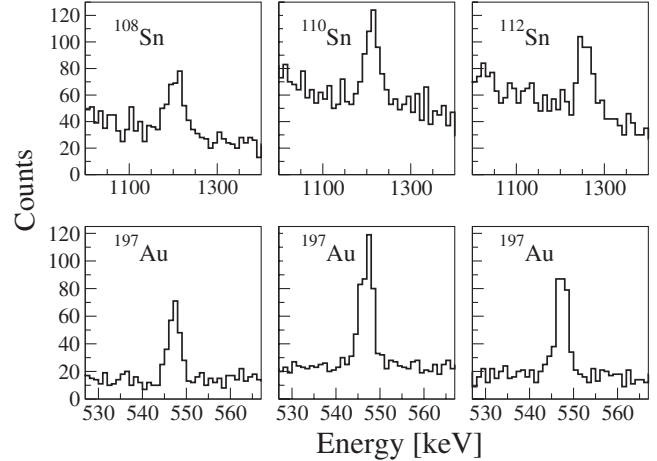


FIG. 1. γ -ray spectra measured by the 90° ring of SeGA for the $^{108-112}\text{Sn}$ projectiles (top) and the corresponding Au target Coulomb excitations (bottom) within the 45 mrad scattering angle in the laboratory reference frame.

tion of the constraints set on the impact parameter and the scattering angles. Taking advantage of the fact that the hardware acceptance of the S800 spectrograph limits the range of the scattering angles for detected events to 60/85 mrad in the dispersive or nondispersive direction, respectively, all the counts corresponding to ^{106}Sn were included in the cross section calculation. For all four isotopes the ratio of the projectile to the target Coulomb excitations was extracted using the data shown in Fig. 2, which had only the hardware gate on angle given by the S800 angular acceptance. The value of these ratios for $^{106-112}\text{Sn}$ are 1.2(3), 1.16(11), 1.24(9), and 1.29(10), respectively. A common scaling factor of 0.19(1) between these ratios and the measured $B(E2, 0_1^+ \rightarrow 2_1^+)$ values was computed for $^{108-112}\text{Sn}$ and applied to the ^{106}Sn ; the resulting $B(E2)$ for ^{106}Sn is reported in Table II. The ^{106}Sn result was obtained in less than ideal conditions, and we cannot safely gate out contributions to the total cross section of processes other than Coulomb scattering. Yet, the measurement gives strong indications that the $B(E2, 0_1^+ \rightarrow 2_1^+)$ is higher than expected for this isotope from structure calculations assuming a stable $Z = 50$ shell gap near ^{100}Sn .

TABLE II. Reduced $E2$ transition rates measured for $^{106-112}\text{Sn}$ isotopes. The results for $^{108-112}\text{Sn}$ correspond to the lab scattering angles smaller than 45 mrad, for the ^{106}Sn the scattering angle limit was set by the hardware S800 spectrograph acceptance [11].

Isotope	$B(E2, 0_1^+ \rightarrow 2_1^+)$ [e^2b^2]	Δ_{stat} [e^2b^2]	Δ_{sys} [e^2b^2]
^{112}Sn	0.240	0.020	0.025
^{110}Sn	0.240	0.020	0.025
^{108}Sn	0.230	0.030	0.025
^{106}Sn	0.240	0.050	0.030

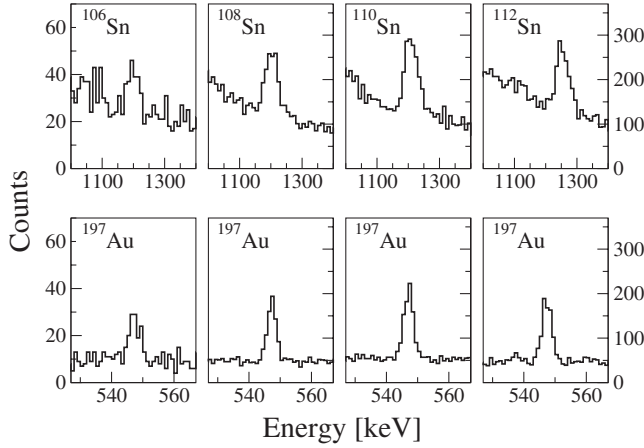


FIG. 2. γ -ray spectra measured with SeGA for the $^{106-112}\text{Sn}$ projectile within the scattering angle limited by the hardware S800 spectrograph acceptance.

Experimental information on the $B(E2, 0_1^+ \rightarrow 2_1^+)$ systematic in Sn isotopes based on the current measurement and Refs. [4–6] is presented in Fig. 3. The asymmetric behavior of the $B(E2)$ with respect to the $N = 66$ neutron midshell at $A = 116$ is in disagreement with several shell-model $B(E2)$ predictions including these from the large-scale shell-model calculations of Refs. [6,7] performed with a ^{90}Zr core. Shell-model calculations consistently predict a $B(E2)$ trend which is nearly parabolic and symmetric with respect to the midshell [6,18]. In regard to other recently proposed theories, the experimental $B(E2)$ strength is underpredicted by the exact pairing model of Ref. [18]. While the predictions of relativistic quasiparticle random phase approximation [19] are consistent with the $B(E2)$ values measured here for the most neutron-deficient

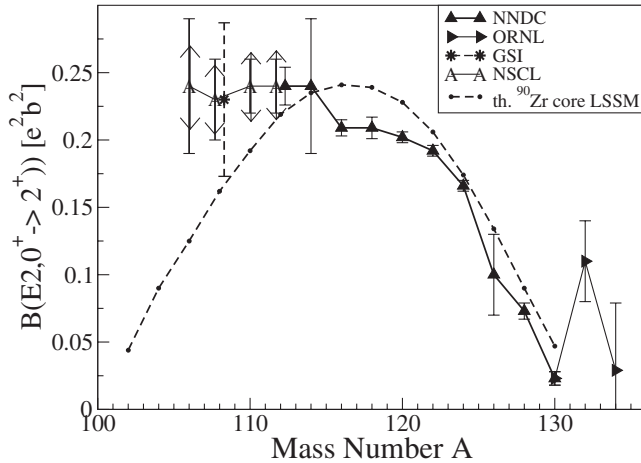


FIG. 3. Experimental data on $B(E2, 0_1^+ \rightarrow 2_1^+)$ in a Sn isotopic chain from the current results for $^{106-112}\text{Sn}$ and from Refs. [4–6]. The dotted line shows the predictions of the large-scale shell-model calculations of Ref. [6] performed with ^{90}Zr core. For $^{108-112}\text{Sn}$ the error bars represent statistical errors; the corresponding systematic errors are marked by arrows. The ^{106}Sn value is tentative, as indicated in the text.

Sn isotopes, the overall trend in the middle of the shell is not well reproduced by these calculations.

The results for $^{100-132}\text{Sn}$ from Refs. [6,7] shown in Fig. 3 were obtained in the $(g_{7/2}, d_{5/2}, d_{3/2}, s_{1/2}, h_{11/2})^{A-100}$ model space for neutrons ($t = 0$) plus up to two-nucleons excited from $g_{9/2}$ to $(g_{7/2}, d_{5/2}, d_{3/2}, s_{1/2}, h_{11/2})$ ($t = 2$) plus up to four protons excited from $g_{9/2}$ to $(g_{7/2}, d_{5/2}, d_{3/2}, s_{1/2})$ (the $t = 4gds$ truncation). The truncation within $t = 4$ is due to computational limitations. It is useful to explore the analogy with $^{56-68}\text{Ni}$ starting with the $(f_{5/2}, p_{3/2}, p_{1/2})^{A-56}$ model space which can be expanded up to the full pf shell. $B(E2)$ values obtained are shown in Fig. 4 as a function of the maximum number of nucleons t excited from $f_{7/2}$. The effective charges are set to $e_p = 1.5$ and $e_n = 0.5$, the same as used in Refs. [6,7] and for Sn calculations in Fig. 3. In comparison with Fig. 3 of Ref. [6], one observes in both cases a large enhancement of the $t = 2$ values over those obtained with $t = 0$. In contrast, the enhancement of $t = 4$ over $t = 2$ for Ni is much larger than the enhancement of $t = 4gds$ compared to $t = 2$ for Sn. For Ni the enhancement becomes larger as one approaches $N = Z$. This asymmetry might be traced to the α -particle-type correlation energies associated with particle-hole excitations near ^{56}Ni . For example, in the full pf shell the wave function for the ^{58}Ni ground state is dominated by the neutron $(f_{5/2}, p_{3/2}, p_{1/2})^2$ ($2p$) configuration, and there is an excited state near 3.5 MeV that is dominated by a four-particle two-hole ($4p2h$) configuration. The $4p2h$ configuration has a $B(E2)$ value that is about 2 orders of magnitude larger than the $2p$ configuration. Thus the mixing of these two configurations that occurs in the full pf wave function gives rise to a large enhancement of the $B(E2, 0_1^+ \rightarrow 2_1^+)$ compared

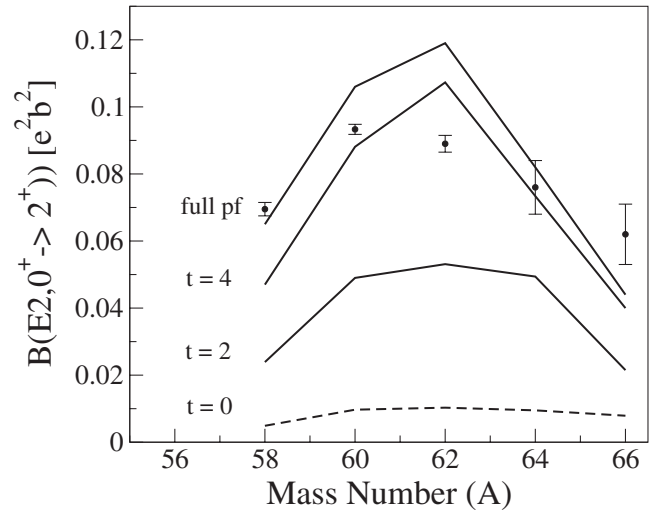


FIG. 4. Experimental data on $B(E2, 0_1^+ \rightarrow 2_1^+)$ in a Ni isotopic chain [4] compared to pf shell-model calculations obtained with the GPDFX1 Hamiltonian [23]. The lines are labeled by the maximum number of nucleons t allowed to be excited out of the $f_{7/2}$ orbit with the full-space results indicated by “full pf ”.

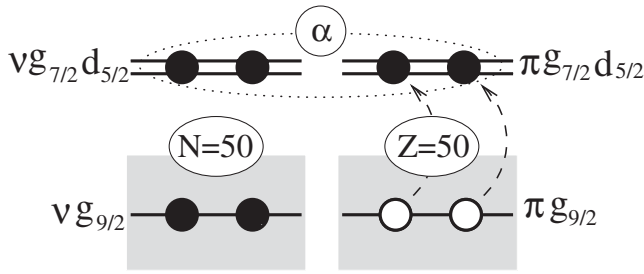


FIG. 5. Schematic representation of proton $2p2h$ excitations across the $Z = 50$ shell gap in ^{102}Sn . The occupation of the same proton and neutron orbitals above the $Z = N = 50$ shell leads to α -like correlations between the valence nucleons.

to the $t = 0$ result. For the $t = 2$ truncation the state dominated by $4p2h$ lies at 5.3 MeV. The $4p2h$ energy converges slowly to 3.5 MeV as a function of increasing t . The situation is similar to that of the $4p4h$ state in ^{56}Ni as shown in Fig. 1 of [20]. The $B(E2, 0_1^+ \rightarrow 2_1^+)$ values slowly converge to their full-space values as a function of the increasing t , as was also shown in Ref. [21].

The analogous $4p2h$ configuration for ^{102}Sn is shown schematically in Fig. 5. The comparison with Ni shows that a test of the Sn isotope calculations would be to investigate the state dominated by $4p2h$ in ^{102}Sn to determine if its energy and mixing with the $2p$ configuration have converged as a function of t . The full α -correlation energies require both proton and neutron excitations, whereas the only four *proton* excitations are allowed by the $t = 4gds$ truncation [7]. The α -correlation energy is enhanced near $N = Z$ when protons and neutrons occupy the same orbitals above the $Z = 50$ core and when the proton and neutron particle states are “open” in the sense that most of the two-particle couplings are allowed. As neutrons are added to ^{100}Sn , the α -correlation energy decreases as the $(g_{7/2}, d_{5/2}, d_{3/2}, s_{1/2})$ configuration becomes more dominated by the closed-shell configuration for $N > 64$.

The excitations across the $Z = 50$ shell gap and α -like correlations discussed above also influence observables other than $B(E2)$'s. The correlations are likely to impact the α -decay rates for nuclei above ^{100}Sn . Next, low-lying 0^+ states in the light Sn isotopes built predominantly on $2p2h$ proton excitations are expected to lie low in energy with collective bands built on top of them. Last, a smooth band termination [22] is expected for these bands due to the limited valence space. All these can be addressed experimentally.

In summary, the measured nearly constant $B(E2)$ strength of $\sim 0.24e^2b^2$ in $^{108-110}\text{Sn}$ isotopes together with the value for the ^{106}Sn $B(E2)$ suggested by the NSCL experiment is in disagreement with the state-of-the-art shell-model predictions. This discrepancy could be explained if $g_{9/2}$ protons from within the $Z = 50$ shell con-

tribute to the structure of low-energy excited states in this region. Such contributions are favored and stabilized by the α -like correlations for protons and neutrons occupying the same shell-model orbitals in nuclei near $N = Z$.

This work is supported by the US NSF No. PHY01-10253, No. PHY-0555366, and No. NSF-MRI PHY-0619407. One author (C.A.) acknowledges the support from the National Science and Engineering Research Council of Canada, the Swedish Foundation for Higher Education and Research, and the Swedish Research Council. The authors acknowledge computational resources provided by the MSU High Performance Computing Center and Center of High Performance Scientific Computing at Central Michigan University.

-
- [1] M. G. Mayer, Phys. Rev. **74**, 235 (1948); **75**, 1969 (1949).
 - [2] O. Haxel, J. H. D. Jensen, and H. E. Suess, Phys. Rev. **75**, 1766 (1949).
 - [3] B. A. Brown *et al.*, Phys. Rev. C **74**, 061303(R) (2006), and references therein.
 - [4] S. Raman, C. W. Nestor, Jr, and P. Tikannen, At. Data Nucl. Data Tables **78**, 1 (2001).
 - [5] D. C. Radford *et al.*, Nucl. Phys. **A752**, 264c (2005).
 - [6] A. Banu *et al.*, Phys. Rev. C **72**, 061305(R) (2005).
 - [7] J. Cederkall, A. Ekstrom, C. Fahlander, and A. M. Hurst *et al.*, Phys. Rev. Lett. **98**, 172501 (2007); Phys. Scr. T **125**, 190 (2006).
 - [8] A. Stolz *et al.*, Nucl. Instrum. Methods Phys. Res., Sect. B **241**, 858 (2005).
 - [9] D. J. Morrissey *et al.*, Nucl. Instrum. Methods Phys. Res., Sect. B **204**, 90 (2003).
 - [10] W. F. Mueller *et al.*, Nucl. Instrum. Methods Phys. Res., Sect. A **466**, 492 (2001).
 - [11] D. Bazin *et al.*, Nucl. Instrum. Methods Phys. Res., Sect. B **204**, 629 (2003).
 - [12] J. Yurkon *et al.*, Nucl. Instrum. Methods Phys. Res., Sect. A **422**, 291 (1999).
 - [13] A. Winther and K. Alder, Nucl. Phys. **A319**, 518 (1979).
 - [14] T. Glasmacher, Annu. Rev. Nucl. Part. Sci. **48**, 1 (1998).
 - [15] J. M. Cook, T. Glasmacher, and A. Gade, Phys. Rev. C **73**, 024315 (2006).
 - [16] A. Gade *et al.*, Phys. Rev. C **68**, 014302 (2003).
 - [17] C. Zhou, Nucl. Data Sheets **76**, 399 (1995).
 - [18] A. Volya and V. Zelevinsky, Nucl. Phys. **A752**, 325 (2005).
 - [19] A. Ansari, Phys. Lett. B **623**, 37 (2005).
 - [20] M. Horoi, B. A. Brown, T. Otsuka, M. Honma, and T. Mizusaki, Phys. Rev. C **73**, 061305(R) (2006).
 - [21] F. Nowacki, Nucl. Phys. **A704**, 223c (2002).
 - [22] A. V. Afanasjev, D. B. Fossan, G. J. Lane, and I. Ragnarsson, Phys. Rep. **322**, 1 (1999).
 - [23] M. Honma, T. Otsuka, B. A. Brown, and T. Mizusaki, Phys. Rev. C **65**, 061301(R) (2002); Phys. Rev. C **69**, 034335 (2004).